

To Control and Optimize the Response of Critical Components of Mandrel

Amol Khot, N. K. Nath, Shailesh Pimple

Abstract: Mandrel is the critical part of the rolling mill operation. Mandrel consists of several components which sometimes encounter unfortunate failures. These components include wedge, mandrel shaft, pull rod or segments. In this thesis design and optimization of wedge and mandrel shaft is carried out. To design the wedge there is need to calculate which the governing parameter while designing of wedge is the 3D modeling and simulation of the wedge is carried out using solid works software. The study also includes the optimization of the shaft. As the mandrel shaft was failed during working so there is need to optimize that shaft. The cause of failure of mandrel shaft was due to fatigue failure. So first of all fatigue failure analysis of shaft is done. For fatigue failure analysis the S-N curve has been created by considering various endurance limit and endurance limit correcting factors. Further study shows that the shaft was susceptible to the fatigue so it needs optimization. By considering various values of the fillet radius optimization is carried out. The shaft is then modeled and simulated in the Ansys v 12.

Index Terms—Ansys, Components, Mandrel, Optimization

I. INTRODUCTION

A. MANDREL

Mandrel is a very important part of rolling mill and strip processing line industry. The mandrels used are of expanding and collapsing type of mandrel to account for the loading and unloading of the coil. When mandrel is used for uncoiling of the coil then it is called uncoiler type mandrel or uncoiler and when this mandrel is used for recoiling of the coil then it is called recoiler type of mandrel or recoiler. Mandrels are capable of providing the high forward tensions that may be required in rolling, as strip as stretch leveled and wound tightly and uniformly on the mandrel drum.

A single mandrel tension reel is generally used at the delivery end of a cold strip reduction mill for strip coiling. The use of such single mandrel tension reels for coiling strip in modern cold strip reduction mills presents a number of problems which are mainly due to the weight of the coils to be handled, tension in the strip and also to the high speeds at which the strip issues from the mill. First, excessive time is required to remove the finished coil from one end of the tension reel. Secondly, mandrel deflection is experienced due to excessive forces over the mandrel length which can create defects in the coil and impose undue wear on the mandrel bearings which support the mandrel at one end. In this regard,

Revised Version Manuscript Received on July 05, 2016.

Amol Khot, Department of Mechanical Engineering, JSPM'S Rajarshi Shahu College of Engineering Tathwade, Pune (Maharashtra), India.

Dr. N. K. Nath, Professor, Department of Mechanical Engineering, JSPM'S Rajarshi Shahu College of Engineering Tathwade, Pune (Maharashtra), India.

Dr. Shailesh Pimple, Associate Professor, Department of Mechanical Engineering, JSPM'S Rajarshi Shahu College of Engineering Tathwade, Pune (Maharashtra), India.

when excessively heavy coils are being wrapped on the tension reel, it is also necessary to provide an outboard bearing support on the normally unsupported end of the tension reel mandrel. In addition, expensive heavy duty mandrel bearings are required to support the coil. Conventional tension reels also require the use of expensive coil stripper equipment to remove the coils from the tension reel mandrel for further processing. Furthermore, where coil sleeves are used, considerable valuable time is consumed in mounting the next sleeve into position endwise over the mandrel.

Matching the rolling and coiling speed and maintaining constant tension in strip are complicated by the changing diameter of the coil as it is being built up. In old mills, the mill motor drives some drums and speeds were matched by slippage in the drive system (as, for example, in slipping clutches). In modern mills, however, the recoilers are driven by variable speed motor, which ensures matched speed at desired tension level. Moreover, in reversing mills, when the strip is being paid off a coiler, the motor acts as a generator returning energy from the back tension to the power supply.

In some instances, additional support for the mandrel is provided by an outboard bearing, which may be moved aside when the coil is to be removed from the mandrel.

Mandrel design for cold mills varies considerably ranging from simple drums no mechanisms for fastening the strip to the mandrel to more elaborate types that clamp the head end of the strip. With the former, a common practice is to fasten the end of the strip onto the drum with a piece of adhesive tape and then rotating the drum to accumulate several wraps on it before applying high tension.

Furthermore the mandrels can also be classified according method used for expansion and collapse of the mandrel. First one is in out wedge type mandrel as shown in fig.1 and other one is quill type mandrel as shown in fig. 2. Generally the in out wedge type mandrel is used for recoiler and quill type mandrel for uncoiler.

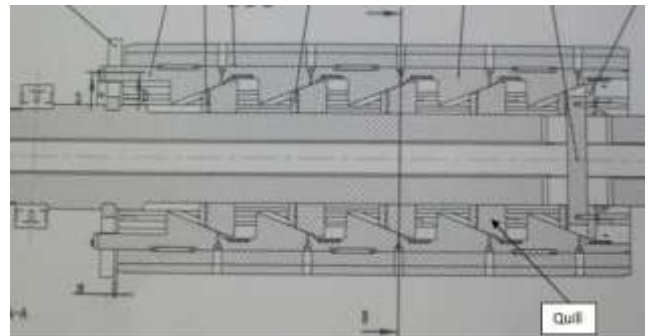


Fig. 1 Quill Type Mandrel

To Control and Optimize the Response of Critical Components of Mandrel

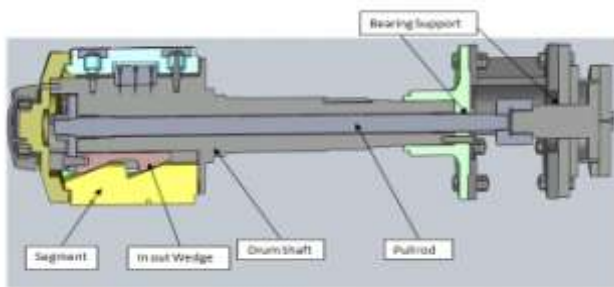


Fig.2 In-out wedge type Mandrel and its Critical Components

B. General Working Principle of Mandrel

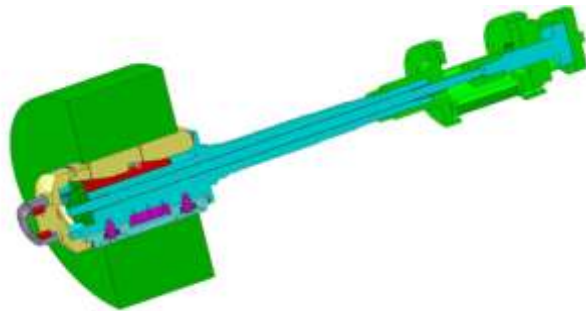


Fig.3 Section of Mandrel

Fig.3. shows the general working of mandrel. A mandrel used in a line processing sheet material and cold rolling includes a segmented drum that is expandable from a contracted position to an expanded position. To enable the drum to accommodate coils of sheet material having different internal diameters, a sleeve consisting of sleeve segments which match the segments of the drum is installed on the drum and is expandable and contractible therewith. A cradle moved by a coil cart is transportable to a position circumscribing the sleeve. The cradle includes magnets, which hold the sleeve in the expanded position after the sleeve is disengaged from the drum, to thereby permit removal of the sleeve. When the sleeve is reinstalled on the drum, the cradle transports the sleeve to its position circumscribing the drum, the drum is then expanded, and the sleeve is secured to the drum, whereupon the cradle is transported away from the drum and sleeve.

II. LITURATURE SURVEY

K.S. Ravi Chandran, P. Chang, G.T. Cashman has presented the paper on competing failure modes and complex S-N curves in fatigue of structural materials. In this paper the author has done research on the failure modes in S-N fatigue, involving surface- and internally-initiated cracks often lead to large variations in fatigue lives. there exists a shorter-life-distribution that is usually associated with surface-crack-initiated failures. There can be a complete separation of the two failure distributions in terms of fatigue life or they can dominate at high and low stress ranges with a discontinuity in fatigue life in the mid-stress-range, depending on the material. He has shown that complex shapes of S-N curves, including the very-high-cycle-fatigue segments can exist due to competing failure modes. Author has presented some examples of competing fatigue failures in steels, titanium alloys and nickel-base super alloys are reviewed.

The above paper helps in creating the S-N curve and determining the theoretical and actual endurance limit for our current project. It also helps in understanding the different regions of the S-N curve. [1]

N.W. Sachs of ASM International presented a paper on Understanding the surface features of fatigue fractures: how they describe the failure cause and the failure history. The paper presented describes the different kind of fracture surface behavior. Also the author has given information about the nature of the fatigue failure. By looking at the failed component how can we interpret that this failure is due to the fatigue. Also he has described about the factors which affect the fatigue failure. And by the influence of a certain parameter how the fatigue failure surface nature changes.[2]

Osman Asi of AfyonKocatepe University has presented a paper on Fatigue failure of a rear axle shaft of an automobile. This paper describes the failure analysis of a rear axle shaft used in an automobile which had been involved in an accident. The axle shaft was found to break into two pieces. The investigation was carried out in order to establish whether the failure was the cause or a consequence of the accident. An evaluation of the failed axle shaft was undertaken to assess its integrity that included a visual examination, photo documentation, chemical analysis, micro-hardness measurement, tensile testing, and metallographic examination. The failure zones were examined with the help of a scanning electron microscope equipped with EDX facility. Results indicate that the axle shaft fractured in reversed bending fatigue as a result of improper welding.[3]

Shuhaizal Bin Mohd Noor of Universiti Malaysia Pahang presented in his study, fracture analysis of a drive shaft of an automobile power transmission system is carried out. Hardness measurements are carried out for each part. For the determination of stress conditions at the failed section, stress analyses are also carried out by the finite element method. The fatigue test experiment had been done to see how long the drive shaft can be stay before had any failure. By compare the hardness number and the properties of material; the driveshaft is making from medium carbon steel. It has higher endurance limit compare to mild steel, brass and aluminum (pure).[4]

III. PROBLEM STATEMENT

There are two problems considered in this thesis.

The first problem is concerned with the wedge type mandrel as shown in fig .2. In the in out wedge type mandrel the wedge governs the expansion and collapse of the mandrel sometimes the wedge of mandrel fails. So there is needed to analyze the wedge and to check whether it will be safe or not. The mandrel was loaded with 26000 kg coil. Another problem is that there is sudden failure of the uncoiler mandrel shaft the quill type mandrel as shown in fig.1 while it is in process. The shaft was fully loaded as the coil of weight 25000 Kg mounted on the mandrel. At the time of failure the shaft was rotating at a speed of 200 rpm. There is need to find out the reason of failure of the shaft and optimize the shaft to avoid further failure of mandrel shaft. The fig.3 shows the failed mandrel shaft.



Fig. 4 Failed Mandrel Shaft

IV. OBJECTIVE

Objective of the project can be stated as

- Analyzing the wedge of the in out wedge type mandrel to avoid the failure of the wedge. Carry out the analysis cases by using solid works.
- Carry out the failure analysis and optimization of the failed shaft of the quill type mandrel to avoid further failure.
- Carry out the analysis of the shaft using ANSYS v12.

V. STRESS CALCULATION FOR SHAFT

The shaft of the uncoiler mandrel is failed so first of all it needs to calculate the various kinds of stresses acting on the mandrel shaft. And to avoid the fatigue failure of shaft these calculated stresses must be compared with the endurance limit.

There are three stresses of concern in this problem

1. Shear from the dead weight
2. Torsion form the strip tension
3. Bending from the cantilevered weight

Coil Diameter = 1800 mm

Eye Diameter = 510 mm

Strip Width = 1300 mm

Tension in the strip = 2000 Kg

Coil Weight = 25000 Kg

$$S_{ut} = 800 \text{ MPa}$$

$$S_{yt} = 600 \text{ MPa}$$

D = Outer Diameter of Shaft = 267 mm

d = Inner Diameter of Shaft = 95 mm

A. Shear Stress from Dead weight of Coil

$$\sigma = \frac{F}{A}$$

$$Area_{@Failure} = \frac{\pi}{4}(D^2 - d^2)$$

$$Area_{@Failure} = \frac{\pi}{4}(267^2 - 95^2)$$

$$Area_{@Failure} = 48902.03 \text{ mm}^2$$

$$\sigma = \frac{27000 * 9.81}{48902.03}$$

$$\sigma = 5.41 \text{ N/mm}^2$$

B. Torsion Stress from Strip Tension

$$\tau = \frac{Tc}{J}$$

T=Torque from strip tension

$$T = \frac{1800}{2} * 20000$$

$$T = 18 * 10^6 \text{ N} - \text{mm}$$

$$J = \frac{\pi}{32}(D^4 - d^4)$$

$$J = \frac{\pi}{32}(267^4 - 95^4)$$

$$J = 490.93 * 10^6 \text{ mm}^4$$

$$c = \frac{267}{2}$$

$$c = 133.5 \text{ mm}$$

$$\tau = \frac{Tc}{J}$$

$$\tau = \frac{18 * 10^6 * 133.5}{490.93 * 10^6}$$

$$\tau = 4.89 \text{ N/mm}^2$$

$$\tau = 4.89 \text{ MPa}$$

C. Bending Stress from Coil Weight:

$$\sigma_b = \frac{M}{I/C}$$

$$\frac{I}{C} = \frac{\pi d^3}{32}$$

$$\frac{I}{C} = \frac{\pi(267)^3}{32}$$

$$\frac{I}{C} = 1.86 * 10^6 \text{ mm}^3$$

Determining the bending moment at the point of failure will require some preliminary calculations. Self-Weight of the shaft is 1340 Kg acting at the center of gravity of the shaft Calculating the reaction forces at the bearing support,

Fig. 5 shows the positions of the bearing support, coil weight and the self-weight of the shaft.

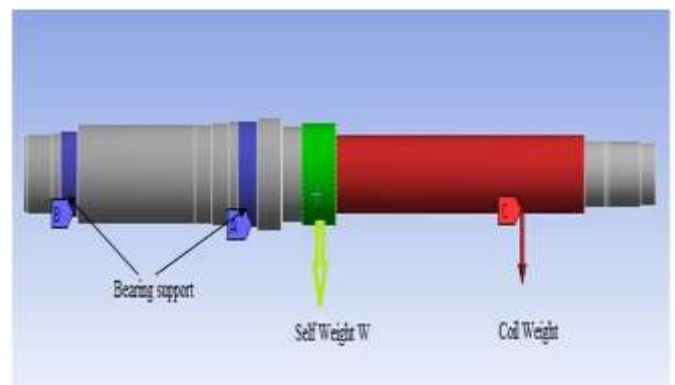


Fig. 5 Constraints and forces on shaft

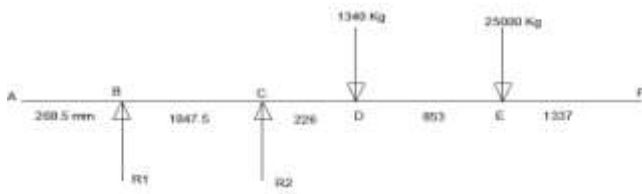


Fig. 6 Shaft Reactions

From fig .6,

Taking Moment about B

$$M_B = 0$$

$$R_2 * 1047.5 - 1340 * 1273.5 - 25000 * 2126.5 = 0$$

$$R_2 = 52380.89 \uparrow Kgf$$

$$\sum F_y = 0$$

$$R_1 + 52380.89 - 1340 - 25000 = 0$$

$$R_1 = 26040.89 \downarrow Kgf$$

Calculating the bending moment at the point of failure, the failure point is at 1585 mm from left end of the shaft.

$$M_{Failure\ point} = 25000 * (2395 - 1585)$$

$$M_{Failure\ point} = 20.25 * 10^7 N - mm$$

$$\sigma_b = \frac{M}{Z}$$

$$\sigma_b = \frac{20.25 * 10^7}{1.86 * 10^6}$$

$$\sigma_b = \frac{202.5}{1.86}$$

$$\sigma_b = 108.87 MPa$$

Because the bending stress is greater than the endurance limit i.e.

$$108.87 > 101.12 MPa$$

The mandrel design is susceptible to fatigue failure.

D. Evaluation of Factor of Safety by using Goodman Theory

In our case the loading is completely reversed loading

So,

$$\sigma_{max} = 108.87 MPa$$

$$\sigma_{min} = -108.87 MPa$$

$$\sigma_m = \frac{\sigma_{max} + \sigma_{min}}{2}$$

$$\sigma_m = \frac{108.87 + (-108.87)}{2}$$

$$\sigma_m = 0$$

$$\sigma_a = \frac{\sigma_{max} - \sigma_{min}}{2}$$

$$\sigma_a = \frac{108.87 - (-108.87)}{2}$$

$$\sigma_a = 108.87 MPa$$

By using Goodman Theory

$$\frac{\sigma_a}{S_e} + \frac{\sigma_m}{S_{ut}} = \frac{1}{n}$$

$$\frac{108.87}{101.12} + 0 = \frac{1}{n}$$

$$n = 0.92$$

$$n < 1$$

As,

n Factor of safety is less than one the design is not safe for fatigue.

E. Evaluating the life of the shaft

Life of the shaft can be calculated from the following data

$$N = \left(\frac{\sigma_a}{a}\right)^{1/b}$$

Where

$$a = \frac{(f S_{ut})^2}{S_e}$$

$$a = \frac{(0.83 * 800)^2}{101.82}$$

$$a = 4330.5$$

$$b = -\frac{1}{3} \log\left(\frac{f * S_{ut}}{S_e}\right)$$

$$b = -\frac{1}{3} \log\left(\frac{0.83 * 800}{101.82}\right)$$

$$b = -0.271$$

Therefore,

$$N = \left(\frac{108.87}{4330.5}\right)^{1/-0.271}$$

$$N = 8 * 10^5 \text{ cycles}$$

The life of the shaft is $8 * 10^5$ cycles only.

F. Selection of Optimum Fillet Radius

For fillet radius 8: Calculating the endurance limit modifying factors for fillet radius of 8 mm. Based on that calculating the endurance limit.

k_a	0.788
k_b	0.7227
k_c	1
k_d	1
k_t	2.19
k_f	2.13
k_e	0.471
S_e	107.73 MPa

For fillet radius 9: Calculating the endurance limit modifying factors for fillet radius of 9 mm. Based on that calculating the endurance limit.

k_a	0.788
k_b	0.7227
k_c	1
k_d	1
k_t	2.02
k_f	1.969
k_e	0.507
S_e	115.67 MPa

For fillet radius 10: Calculating the endurance limit modifying factors for fillet radius of 10 mm. Based on that calculating the endurance limit.

k_a	0.788
-------	-------

From above calculations and tables it is clear that the providing a fillet radius of 10 mm is best for the shaft to live for infinite number of cycles.

3D Modeling and Finite Element Analysis of Shaft

VI. ANALYTICAL MODELING

The 3D modeling of the failed shaft is done in the GUI of the ANSYS Workbench V12. As shown in the fig. 7 the arrow pointed area is our failure zone. The fillet radius provided at the failure step is of 7 mm.

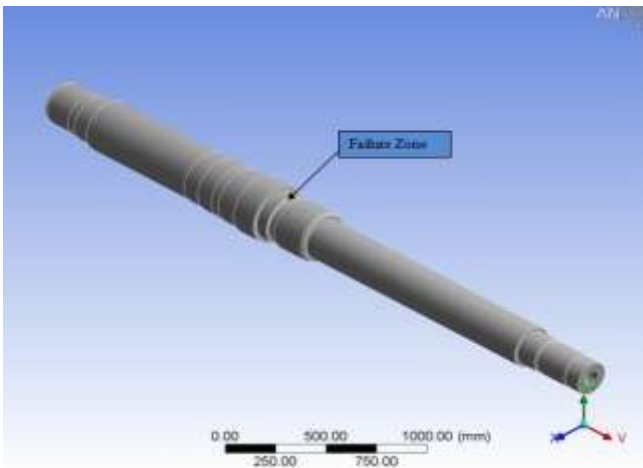


Fig. 7 3D Shaft Model

A. Meshing

The above 3D model of the shaft has been meshed in the ANSYS v12. The meshing used is the solid mesh. Here we are using 2nd order tetrahedron element means the midside nodes in the element are kept. Which is obviously increases the accuracy of the solution.

- Type of Element: Tetrahedron
- No. of Nodes: 1036581
- No. of Elements: 725001
- Mid side Node: Kept
- Element size: 13 mm

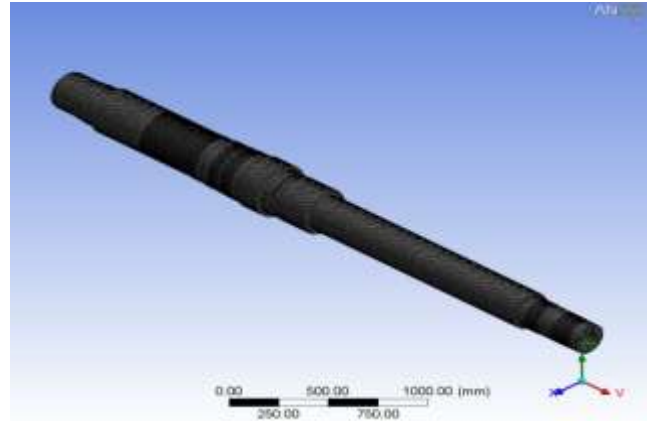


Fig. 8 Meshed 3D Shaft Model

B. Constraints and Forces:

The mandrel shaft is supported on two spherical roller bearings. For doing the static structural analysis we are considering these two supports as fixed. That is shown in fig.8

The force applied on the shaft is the weight of the coil total weight of the coil is 25 Tonne. This weight of coil is exerted on the segment area of the mandrel shaft. Force on shaft is shown in the fig. 9

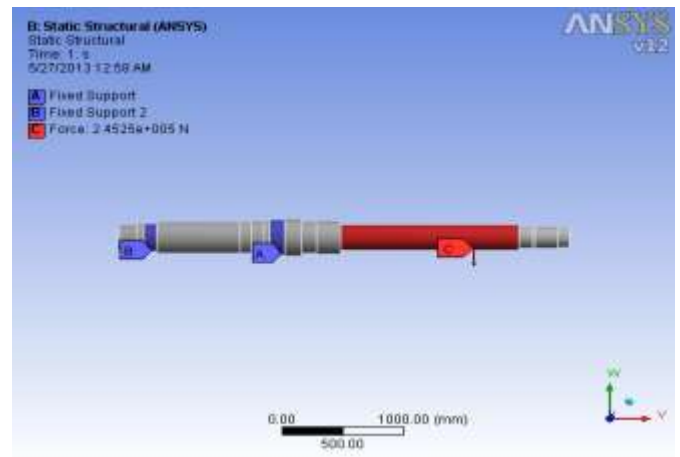


Fig. 9 Constraints and forces on Shaft

Material Specifications:

The material used in this analysis is EN24 having following properties

- Yield Strength=600 MPa
- Ultimate Tensile Strength = 800 MPa
- Young's Modulus of Elasticity= 210 GPa
- Poisson's ratio = 0.32
- Mass Density = 7850 Kg/m³

C. Stresses:

After applying the constraints and forces the 3D model of shaft has been solved for static structural analysis in ANSYS v12. The solution of the von-Mises stresses has been shown in the following fig 7.4. From the fig 7.4 we can get to know that the maximum stresses coming in the shaft are at the same location where the actual failure of the shaft occurred.

- Max. Stress= 205.64 Mpa
- Min. Stress= 2.7e-7 Mpa



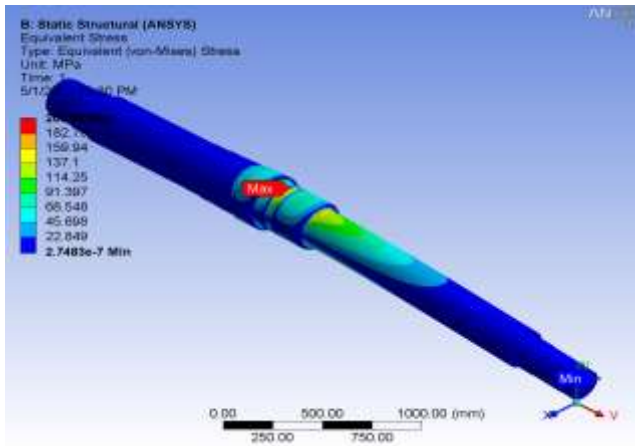


Fig. 10 Von Mises stresses on Shaft

D. Deflection:

The deflection in the mandrel shaft is as shown in the following fig. 11

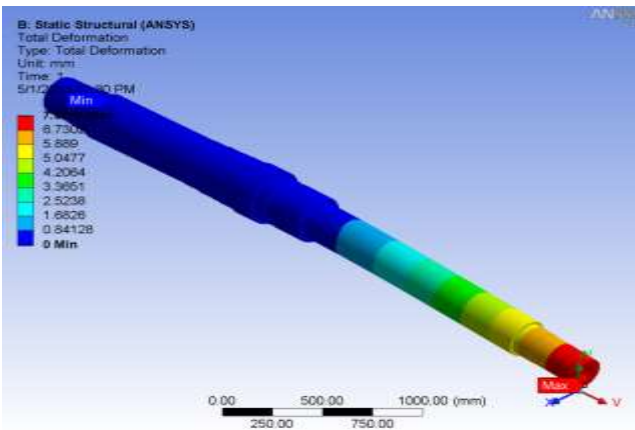


Fig. 11 Deflection of Mandrel

VII. RESULTS AND CONCLUSION

A. Wedge Analysis Results:

In the analysis of the wedge it is found that the if we replace the current combination of the wedge liner and base metal from al bronze, cast alloy steel to al bronze, alloy steel then there is 10% decrease in the deformation of the wedge
The Von Mises stresses are well below the yield strength of the material.

- The best combination of liner thickness and penetration of it into base material is 9 mm thick liner and 8 mm.

B. Optimization of shaft results

1. Analytical Results:

TABLE I. Fillet Radius and Endurance Limit

Fillet Radius	Endurance Limit
7	101.82
8	107.73
9	115.67
10	116.63
16	136.08

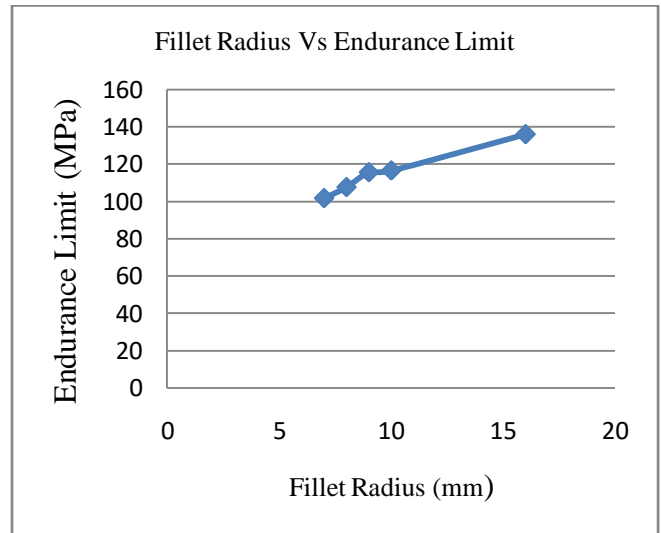


Fig. 12. Fillet Radius Vs Endurance Limit

2. ANSYS Results:

- Ansys result shows that the maximum stresses coming in the shaft are at the step or the region where the actual failure of shaft occurred
- As the maximum stresses showed by the ansys are about 205 MPa. This is because there is geometric discontinuity in the shaft.
- This geometric discontinuity is not considered by the software while solving for the maximum stresses. As the solver shows results for a max stresses but these max stresses coming in the component are for just for one or two nodes and these high stresses are due to the distortion of the element occurring at the stress concentration area.
- To account for this geometric discontinuity or stress concentration we need to plot the graph of stress Vs nodal distance.
- From the following graph the actual stress developed in shaft are about 118 MPa.

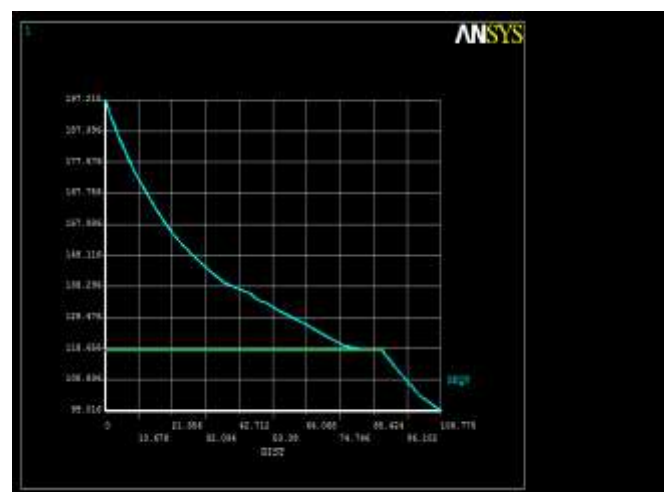


Fig. 13 Stress Vs Nodal Distance

- The following graph shows the variation of the maximum stresses in the shaft with respect to the fillet radius



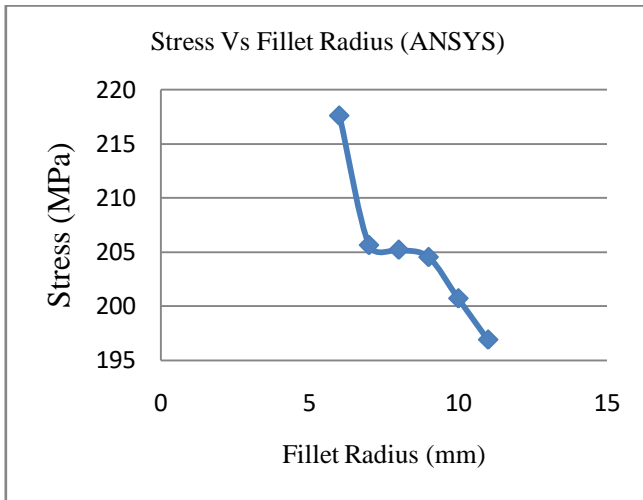


Fig. 14 Stress Vs Fillet Radius

- The current study shows that the endurance limit or fatigue strength of the mandrel shaft in quill type mandrel can be increased by increasing the fillet radius at the step. But this can also be achieved by increasing the surface finish of the shaft or making the shaft grounded but this increases the cost of the shaft. Secondly we can remove the step and we can increase the fatigue strength but it will change the whole design of the shaft and at this point it is not feasible. So we have gone for the changing the fillet radius.
- The studies executed in the scope of both stress and fatigue analyses of the mandrel shaft have revealed the following.
- The analytical calculation shows that the shaft is susceptible to the fatigue failure.
- The currently provided fillet radius of 7 mm at the step is not enough to account for fatigue.
- The fillet radius must be modified to the 10 mm, to account for fatigue, to have factor of safety in fatigue more than one.
- The analytical calculation shows that there is failure of the shaft at the step as the induced bending stresses in the shaft are more than the endurance limit.
- The major factor that is controlling the stresses at the step is the fillet radius provided at the step.
- If we go on increasing the fillet radius there is considerable increase in the endurance limit.
- The following graph fig. 12 shows the variation of endurance limit with respect to the change in fillet radius. The graph shows that as we go on increasing the fillet radius the corresponding endurance limit goes on increasing. Max. Deflection= 7.31 mm Min. Deflection=0

REFERENCES

1. Sandip Bhattacharyya —Failure analysis of gas blower shaft of a blast furnacel- Engineering Failure Analysis 15 (2008) 349–355
2. Osman Asi Fatigue failure of a rear axle shaft of an automobile-Engineering Failure Analysis 13 (2006) 1293–1302
3. E. Rusiński, J. Czmochowski, P. Moczko — Failure reasons investigations of dumping conveyor breakdown- Volume 23 Issue 1 July 2007Journal of Achievements in Materials and Manufacturing Engineering
4. K. Solanki , M.F. Horstemeyer —Failure analysis of AISI 304 stainless steel shaftl - Engineering Failure Analysis 15 (2008) 835–846
5. Shuhaizal bin mohdnoor-failure analysis of driveshaft of toyotaseg university of Malaysia Pahang, 2007-08

6. William L. Roberts (1978), “Cold Rolling of Steels.”, Marcel Dekker Inc. New York.
7. A. K. Dutta, G. Das, P. K. De, P. Ramachandrarao (2006), “Finite Element Modelling of rolling process and optimization of process parameter” , Material Science and Engineering, Page no.11-20.